

Blood Flow Through a Catheterized Artery Having a Mild Stenosis at the Wall with a Blood Clot at the Centre

Anber Saleem^{1,2}, Salman Akhtar³, Sohail Nadeem^{3,*}, Alibek Issakhov⁴ and Mehdi Ghalambaz^{5,6}

¹Mathematics and Its Applications in Life Sciences Research Group, Ton Duc Thang University, Ho Chi Minh City, Vietnam

²Faculty of Mathematics and Statistics, Ton Duc Thang University, Ho Chi Minh City, Vietnam

³Department of Mathematics, Quaid-i-Azam University, Islamabad, 45320, Pakistan

⁴Al-Farabi Kazakh National University, Faculty of Mechanics and Mathematics, av. al-Farabi, 71, Almaty, Kazakhstan

⁵Institute of Research and Development, Duy Tan University, Da Nang City, 550000, Vietnam

⁶Faculty of Electrical–Electronic Engineering, Duy Tan University, Da Nang City, 550000, Vietnam

*Corresponding Author: Sohail Nadeem. Email: sohail@qau.edu.pk

Received: 03 June 2020; Accepted: 07 August 2020

Abstract: The blood flow through a catheterized artery having a mild stenosis at the wall together with a blood clot at the centre is studied in the current investigation. Stenosis can occur in vessels carrying blood to brain (i.e., Carotid arteries), Renal arteries that supply blood to kidneys etc. The flow is refined in such vessels by application of catheter. We have used a Newtonian viscous fluid model and also distinct shapes of stenosis, (i.e., symmetric and non-symmetric shapes) are considered for this study. The entropy generation together with viscous dissipation is also taken into account for a complete description of heat transfer mechanism. Exact solutions are calculated for the problem subject to given “no slip conditions”. The results are discussed graphically. The velocity quickly increases for a non-symmetric stenosis as compared to a symmetric stenosis. When the height of mild stenosis increases and the channel becomes narrow then the velocity increases in the centre but it decreases with the stenosed wall. However, as the height of blood clot σ increases then the velocity of blood flow reduces with the wall having clot but it remains almost same with the stenosed wall. Streamlines are plotted to visualize the flow pattern. The trapping is symmetric for a symmetric stenosis shape but it changes to non-symmetric trapping when we have a non-symmetric shape of stenosis.

Keywords: Blood flow; catheter; stenosed artery; blood clot; entropy

Nomenclature

| | |
|------------------------|---------------------------------------|
| (\bar{r}, \bar{z}) : | Cylindrical coordinate system; |
| (u, w) : | Radial and axial velocity components; |
| R : | Non-stenotic radius of capillary; |
| cR : | Radius of catheter (inner tube); |
| b : | Stenosis length; |



This work is licensed under a Creative Commons Attribution 4.0 International License, which permits unrestricted use, distribution, and reproduction in any medium, provided the original work is properly cited.

| | |
|--------------|---|
| $n \geq 2$: | Shape parameter of stenosis; |
| $n = 2$: | Symmetric stenosis shape; |
| \bar{T} : | Temperature of fluid; |
| μ_f : | Dynamic viscosity; |
| σ : | Maximum height of clot; |
| z_d : | Axial displacement of clot; |
| B_r : | Brickmann number; |
| θ_0 : | Dimensionless ratio of absolute to characteristic temperature difference; |
| δ^* : | Stenosis maximum height; |
| a : | Stenosis location; |
| $n = 6$: | Asymmetric stenosis shape; |
| L : | Length of tube; |
| u_0 : | Characteristic velocity; |

1 Introduction

Stenosis is an arterial disease that results in narrowing of blood vessel due to collection of plaque on the wall of arteries. It reduces the flow of blood and the situation gets worse when this stenosis also produces a thrombus within the vessel, (i.e., a blood clot is formed inside the artery). In this scenario, the flow through such diseased arteries is improved by using a catheter. The blood flow problem for an artery having stenosed walls was explained by Ponalagusamy [1]. It has attracted the interest of many researchers and this topic is further mathematically interpreted due to its medical and biological uses. Further, stenosis can occur in vessels carrying blood to brain (i.e., Carotid arteries), Renal arteries that supply blood to kidneys etc. Chaturani et al. [2] had used a non-Newtonian model of fluid flow to illustrate the blood flow inside a stenosed artery. Moreover, the stenosed artery study is examined for many different fluid models that cover the non-Newtonian properties of blood flow problems. The blood flow through stenosed arteries for various fluid models is given in the studies [3–5]. A thrombus may also be developed in such arteries with stenosis and to cover this aspect mathematically, the blood flow inside a diseased artery having both stenosis and thrombus was studied by Doffin et al. [6]. They had used a Newtonian fluid model and provided both theoretical and experimental results in their work. Srivastava et al. [7] had discussed the blood flow inside a catheterized vessel having stenosed walls. The surgical method for catheter injection inside a composite stenosed artery was explained by Mekheimer et al. [8]. They had provided a mathematical model to explain the blood flow between eccentric tubes. Ramana Reddy et al. [9] had conveyed the mathematical description for blood flow inside a diseased artery by using a catheter. They had considered different shapes of stenosis in their theoretical investigation. By inspecting the available study of literature work, It is uncovered that the blood flow inside a catheterized artery having a mild stenosis at the wall together with a blood clot at the centre of artery is not examined mathematically by anyone. We have considered distinct shapes of stenosis, (i.e., combine results for symmetric and asymmetric shapes) for the first time in the literature. The irreversibility study is also main focus of this work and entropy generation is considered for this work.

The heat transfer phenomenon also has significant importance in fluid flow problems. Bhatti et al. [10] had interpreted the heat transfer of blood flow inside a diseased artery having a thrombus. The unsteady flow and heat transfer mechanism through a catheterized vessel with stenosis was discussed by Ahmed et al. [11]. Entropy generation together with viscous dissipation has significant importance in heat transfer phenomenon. Entropy is defined as the chaos and disturbance in a system. Akbar et al. [12] had illustrated the entropy generation for an annulus

problem with endoscopic effects. The blood flow through a stenosed artery using a Newtonian fluid model with entropy generation was explained by Akbar et al. [13].

In the present work, we have studied the blood flow inside a catheterized artery having a mild stenosis at the wall together with a blood clot at the centre of artery. We have used a Newtonian viscous fluid model and distinct shapes of stenosis, (i.e., symmetric and non-symmetric shapes) are considered for this study. The entropy generation together with viscous dissipation is also considered. Exact solutions are calculated for the problem subject to given “no slip conditions.” The solution is discussed and help is taken from [14]. The results are explained graphically. Streamlines are plotted to see the details of flow.

2 Mathematical Formulation

Consider blood flow inside a catheterized artery having a stenosed wall and a blood clot at the centre (Fig. 1).

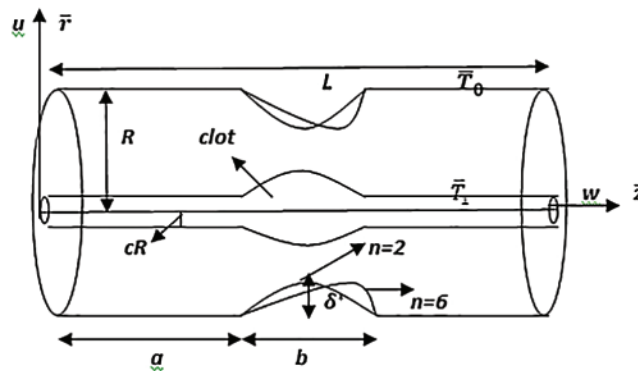


Figure 1: Geometry of the problem

The geometry of outer wall (i.e., stenosis wall) $\bar{\eta}(z)$, and inner wall (i.e., clot wall) $\bar{\epsilon}(z)$, in dimensional form are defined by [15]

$$\bar{\eta}(z) = \begin{cases} R[1 - K \{b^{n-1}(\bar{z} - a) - (\bar{z} - a)^n\}], & a \leq \bar{z} \leq a + b \\ R & \text{otherwise} \end{cases}, \quad (1)$$

$$\bar{\epsilon}(z) = \begin{cases} R[c + f_1(\bar{z})], & a \leq \bar{z} \leq a + b \\ cR & \text{otherwise} \end{cases}, \quad (2)$$

where $f_1(\bar{z})$ defines the geometry of clot and its shape is handled by an appropriate choice of $f_1(\bar{z})$. Moreover, the value of K is given by

$$K = \frac{\delta^*}{Rb^n} \frac{n^{\frac{n}{n-1}}}{n-1}, \quad (3)$$

Here δ^* defines the maximum height attain by stenosis at $z = a + \frac{b}{n^{n-1}}$. The shape of stenosis varies with changing values of parameter n . For $n=2$, the stenosis is symmetric in shape but for $n=6$, it is not symmetric anymore. The governing equations in dimensional form are

$$\frac{1}{\bar{r}} \frac{\partial(\bar{r}\bar{u})}{\partial\bar{r}} + \frac{\partial\bar{w}}{\partial\bar{z}} = 0, \quad (4)$$

$$\rho \left[\bar{u} \frac{\partial\bar{u}}{\partial\bar{r}} + \bar{w} \frac{\partial\bar{u}}{\partial\bar{z}} \right] = -\frac{\partial\bar{p}}{\partial\bar{r}} + \mu \left[\frac{\partial^2\bar{u}}{\partial\bar{r}^2} + \frac{1}{\bar{r}} \frac{\partial\bar{u}}{\partial\bar{r}} + \frac{\partial^2\bar{u}}{\partial\bar{z}^2} - \frac{\bar{u}}{\bar{r}^2} \right], \quad (5)$$

$$\rho \left[\bar{u} \frac{\partial\bar{w}}{\partial\bar{r}} + \bar{w} \frac{\partial\bar{w}}{\partial\bar{z}} \right] = -\frac{\partial\bar{p}}{\partial\bar{z}} + \mu \left[\frac{\partial^2\bar{w}}{\partial\bar{r}^2} + \frac{1}{\bar{r}} \frac{\partial\bar{w}}{\partial\bar{r}} + \frac{\partial^2\bar{w}}{\partial\bar{z}^2} \right], \quad (6)$$

$$\rho C_p \left[\bar{u} \frac{\partial\bar{T}}{\partial\bar{r}} + \bar{w} \frac{\partial\bar{T}}{\partial\bar{z}} \right] = k \left[\frac{\partial^2\bar{T}}{\partial\bar{r}^2} + \frac{1}{\bar{r}} \frac{\partial\bar{T}}{\partial\bar{r}} + \frac{\partial^2\bar{T}}{\partial\bar{z}^2} \right] + \mu \left[2 \left\{ \left(\frac{\partial\bar{u}}{\partial\bar{r}} \right)^2 + \left(\frac{\bar{u}}{\bar{r}} \right)^2 + \left(\frac{\partial\bar{w}}{\partial\bar{z}} \right)^2 \right\} + \left(\frac{\partial\bar{w}}{\partial\bar{r}} + \frac{\partial\bar{u}}{\partial\bar{z}} \right)^2 \right], \quad (7)$$

The governing equations are simplified by considering following non-dimensional variables

$$r = \frac{\bar{r}}{R}, \quad z = \frac{\bar{z}}{b}, \quad w = \frac{\bar{w}}{u_0}, \quad u = \frac{L\bar{u}}{u_0\delta^*}, \quad p = \frac{R^2\bar{p}}{u_0b\mu_f}, \quad \theta = \frac{\bar{T} - \bar{T}_0}{\bar{T}_1 - \bar{T}_0}, \quad \epsilon(z) = \frac{\bar{\epsilon}(z)}{R},$$

$$\eta(z) = \frac{\bar{\eta}(z)}{R}, \quad h = \frac{a}{b}, \quad \delta = \frac{\delta^*}{R}, \quad Br = \frac{\mu_f u_0^2}{k_f(\bar{T}_1 - \bar{T}_0)}, \quad S_{G_0} = \frac{k_f(\bar{T}_1 - \bar{T}_0)^2}{\bar{T}_0^2 R^2},$$

$$\theta_0 = \frac{\bar{T}_0}{(\bar{T}_1 - \bar{T}_0)}.$$

The following assumptions are considered to deal with a mild stenosis case

$$\delta = \frac{\delta^*}{R} \ll 1, \quad \frac{Rn^{\frac{1}{n-1}}}{b} \sim o(1) \quad (9)$$

Using the dimensionless variables given in Eq. (8) and the assumptions for a mild stenosis given in Eq. (9), in Eqs. (4)–(7), the dimensionless equations are given as

$$\frac{\partial p}{\partial r} = 0, \quad (10)$$

$$\frac{\partial p}{\partial z} = \frac{\partial^2 w}{\partial r^2} + \frac{1}{r} \frac{\partial w}{\partial r}, \quad (11)$$

$$\frac{\partial^2 \theta}{\partial r^2} + \frac{1}{r} \frac{\partial \theta}{\partial r} + Br \left(\frac{\partial w}{\partial r} \right)^2 = 0, \quad (12)$$

The corresponding boundary conditions are

$$w = 0, \quad \text{at } r = \epsilon(z), \quad \text{and } w = 0, \quad \text{at } r = \eta(z), \quad (13)$$

$$\theta = 1, \quad \text{at } r = \epsilon(z), \quad \text{and } \theta = 0, \quad \text{at } r = \eta(z), \quad (14)$$

The geometries of outer wall $\eta(z)$ and the inner wall $\epsilon(z)$ are given in dimensionless form. The function $f_1(\bar{z})$ is suitably selected [15] to describe the clot model.

$$\eta(z) = \begin{cases} 1 - \delta \frac{n}{n-1} [(z-h) - (z-h)^n], & h \leq z \leq h+1 \\ 1 & \text{otherwise} \end{cases} \quad (15)$$

$$\epsilon(z) = \begin{cases} c + \sigma e^{-\pi^2(z-z_d-0.5)^2}, & h \leq z \leq h+1 \\ c & \text{otherwise} \end{cases} \quad (16)$$

3 Exact Solution

The exact solution is obtained for velocity profile by solving Eq. (11), subject to boundary conditions given in Eq. (13)

$$w = \frac{\left[\frac{\partial p}{\partial z} \left\{ (-\epsilon^2 + \eta^2) \text{Log}(r) + (r^2 - \eta^2) \text{Log}(\epsilon) + (-r^2 + \epsilon^2) \text{Log}(\eta) \right\} \right]}{4(\text{Log}(\epsilon) - \text{Log}(\eta))}, \quad (17)$$

The volumetric flow rate is calculated by using

$$Q = \int_{\epsilon}^{\eta} r w \, dr, \quad (18)$$

Thus the expression for pressure gradient is calculated

$$\frac{dp}{dz} = \frac{16Q(\text{Log}(\epsilon) - \text{Log}(\eta))}{(\epsilon^2 - \eta^2) [-\epsilon^2 + \eta^2 + (\epsilon^2 + \eta^2) (\text{Log}(\epsilon) - \text{Log}(\eta))]}, \quad (19)$$

The wall shear stress τ_w is evaluated as

$$\tau_w = - \left. \frac{\partial w}{\partial r} \right|_{r=\eta} = \frac{- \frac{\partial p}{\partial z} \left[\frac{-\epsilon^2 + \eta^2}{\eta} + 2\eta(\text{Log}(\epsilon) - \text{Log}(\eta)) \right]}{4(\text{Log}(\epsilon) - \text{Log}(\eta))}, \quad (20)$$

The temperature profile is obtained by evaluating Eq. (12), subject to corresponding boundary conditions given in Eq. (14)

$$\begin{aligned}
\theta = & \frac{1}{64(\text{Log}(\epsilon) - \text{Log}(\eta))^2} \left[-2B_r \left(\frac{\partial p}{\partial z} \right)^2 (\epsilon^2 - \eta^2)^2 (\text{Log}(r))^2 - B_r \left(\frac{\partial p}{\partial z} \right)^2 (r^2 - \eta^2) \right. \\
& \times \text{Log}(\epsilon) \left\{ -4(\epsilon^2 - \eta^2) + (r^2 + \eta^2) \text{Log}(\epsilon) \right\} + \left\{ -4B_r \left(\frac{\partial p}{\partial z} \right)^2 (r^2 - \epsilon^2) (\epsilon^2 - \eta^2) + (-64 + B_r \right. \\
& \times \left. \left. \left(\frac{\partial p}{\partial z} \right)^2 (2r^4 - 3\epsilon^4 + 4\epsilon^2\eta^2 - 3\eta^4) \right) \text{Log}(\epsilon) \right\} \text{Log}(\eta) + \left(64 + B_r \left(\frac{\partial p}{\partial z} \right)^2 (-r^4 + \epsilon^4) \right) \\
& \times (\text{Log}(\eta))^2 + \text{Log}(r) \left\{ -4B_r \left(\frac{\partial p}{\partial z} \right)^2 (\epsilon^2 - \eta^2)^2 + \left(64 + B_r \left(\frac{\partial p}{\partial z} \right)^2 (3\epsilon^4 - 4\epsilon^2\eta^2 + \eta^4) \right) \right. \\
& \left. \times \text{Log}(\epsilon) + \left(-64 + B_r \left(\frac{\partial p}{\partial z} \right)^2 (\epsilon^4 - 4\epsilon^2\eta^2 + 3\eta^4) \right) \text{Log}(\eta) \right\} \left. \right]. \quad (21)
\end{aligned}$$

4 Entropy Generation Analysis

The dimensional volumetric entropy generation is given [16]

$$S_G = \frac{k_f}{T_0^2} \left[\left(\frac{\partial \bar{T}}{\partial \bar{r}} \right)^2 + \left(\frac{\partial \bar{T}}{\partial \bar{z}} \right)^2 \right] + \frac{\mu_f}{T_0} \left[2 \left\{ \left(\frac{\partial \bar{u}}{\partial \bar{r}} \right)^2 + \left(\frac{\bar{u}}{\bar{r}} \right)^2 + \left(\frac{\partial \bar{w}}{\partial \bar{z}} \right)^2 \right\} + \left(\frac{\partial \bar{w}}{\partial \bar{r}} + \frac{\partial \bar{u}}{\partial \bar{z}} \right)^2 \right], \quad (22)$$

Using the dimensionless variables given in Eq. (8) and the assumptions given in Eq. (9), the dimensionless form of entropy generation is provided

$$N_S = \frac{S_G}{S_{G_0}} = \left(\frac{\partial \theta}{\partial r} \right)^2 + \theta_0 B_r \left(\frac{\partial w}{\partial r} \right)^2, \quad (23)$$

Eq. (23) consists of two parts, the entropy generation due to finite temperature difference ($N_{S_{cond}}$) is given in first part while the entropy generation due to viscous effects ($N_{S_{visc}}$) is given in second part. The entropy generation profile is completed together with velocity and temperature profiles. Thus the convective heat transfer mechanism is fully explained by it. The Bejan number is computed with the following formula [17]

$$B_e = \frac{N_{S_{cond}}}{N_{S_{cond}} + N_{S_{visc}}} = \frac{\left(\frac{\partial \theta}{\partial r} \right)^2}{\left(\frac{\partial \theta}{\partial r} \right)^2 + \theta_0 B_r \left(\frac{\partial w}{\partial r} \right)^2}. \quad (24)$$

5 Results and Discussion

The graphical results are discussed for exact solutions obtained in previous section. The symmetric shape of mild stenosis (i.e., for $n = 2$) and the non-symmetric shape (i.e., for $n = 6$) both are considered for accomplishing the graphical results. Thus, we have plotted combine graphs for both symmetric and non-symmetric shapes of stenosis. In real blood flow problems, one can have the details for velocity of flow, temperature, disorder by means of entropy study against various sizes of stenosis as well as thrombus. Moreover, the main purpose is to refine the flow that is confined due to presence of stenosis and thrombus. Thus, all these graphical results are helpful for this purpose, as they clearly depict the variations of velocity, temperature etc against certain parameters. Figs. 2a–2d, represent the velocity profile for distinct values of various physical parameters that are involved. Fig. 2a show that there is increase in velocity as the value of δ increases for both cases $n = 2$, and $n = 6$. It means that as the height of mild stenosis increases and the channel becomes narrow then the velocity increases in the centre but it decreases with the stenosis wall. The velocity gains magnitude for enhancing values of Q in both cases, as depicted in Fig. 2b. It is certain that the velocity increments by increasing the flow rate. Fig. 2c shows that there is decline in velocity profile with enhancing values of σ for both cases. It yields, as the height of blood clot σ enhances then the velocity of blood flow reduces with the wall having clot but it remains almost same with the stenosis wall. There is increase in the velocity with increasing values of z_d , as represented in Fig. 2d. These graphical results also convey that the velocity quickly increases for a non-symmetric stenosis as compared to a symmetric stenosis. Figs. 3a–3d are plotted to reveal the effects of distinct physical parameters on the temperature profile. Fig. 3a reveals that the temperature profile increases by increasing the value of B_r , for both cases. It means that viscous dissipation is generating more heat as compared to heat transferred by conduction. There is decline in the temperature with increasing values of δ , as depicted in Fig. 3b. Fig. 3c depicts that there is increase in temperature with increasing flow rate Q for both cases. The temperature increases with incrementing values of σ , as shown in Fig. 3d. Figs. 4a–4d convey the effects of distinct parameters on wall shear stresses against the axial coordinate z . Fig. 4a reveals that τ_w increases with increasing values of δ . (i.e., there is more resistance to flow at the wall with stenosis, when the height of stenosis enhance). The wall shear stresses τ_w also increase by increasing the rate of flow Q , as shown in Fig. 4b. The main reason for this increase in the value of τ_w is the “no slip condition” at the boundaries. Fig. 4c reveals that τ_w increases with increasing values of σ . Clearly, wall shear stresses increase with increasing clot height. There is decline in the value of τ_w , as the value of z_d enhances, as shown in Fig. 4d. The entropy generation is plotted for B_r and θ_0 , as shown in Figs. 5a, 5b respectively. Fig. 5a reveals that there is decline in entropy with the wall having thrombus but entropy increases with the wall having stenosis for increasing values of B_r , in both cases of symmetric and non-symmetric shapes of stenosis. The value of entropy N_s increments with increasing values of θ_0 , as given in Fig. 5b. Both graphs reveal that entropy is minimum near about the centre of channel, since disorder is minimum at centre. Thus the chaos and disturbance in the system gains magnitude with increasing temperature. Figs. 6a, 6b are plotted to study the effects of B_r and θ_0 on Bejan number. Fig. 6a shows that the value of B_e declines with the wall having thrombus but increases with the wall having stenosis, for increasing values of B_r . Further, it's value is minimum near about the centre. Fig. 6b reveals that there is decline in Bejan number with increasing values of θ_0 . Streamlines are plotted for various values of flow rate Q , considering both cases of symmetric (i.e., $n = 2$) and non-symmetric (i.e., $n = 6$) shapes of stenosis, as shown in Figs. 7a–7d. The symmetric and non-symmetric shapes of stenosis can be seen clearly in these graphs. Figs. 7e–7h also show the streamlines for distinct values of σ , again considering both cases of symmetric and non-symmetric

shapes of stenosis. The variation in the height of thrombus together with different shape stenosis can be seen clearly in these graphs. Further, the trapping is symmetric for a symmetric stenosis shape but it changes to non-symmetric trapping when we have a non-symmetric shape of stenosis.

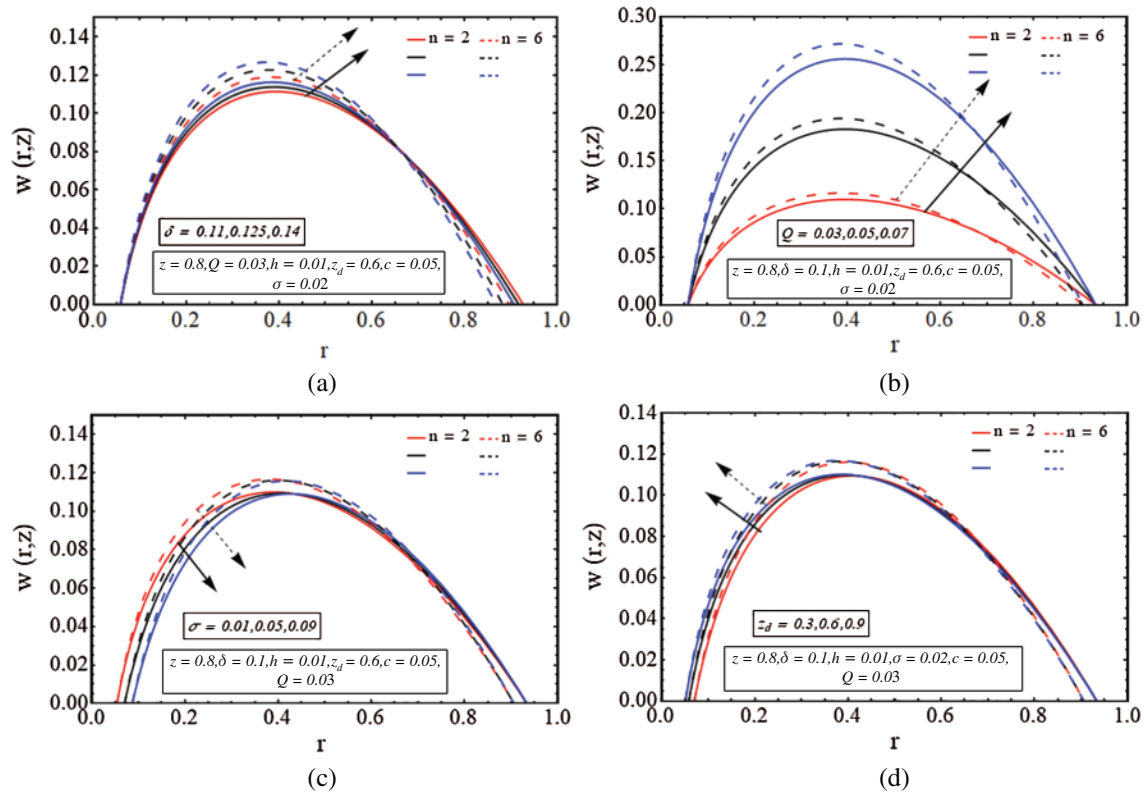


Figure 2: (a) Velocity profile for δ . (b) Velocity profile for Q . (c) Velocity profile for σ . (d) Velocity profile for z_d

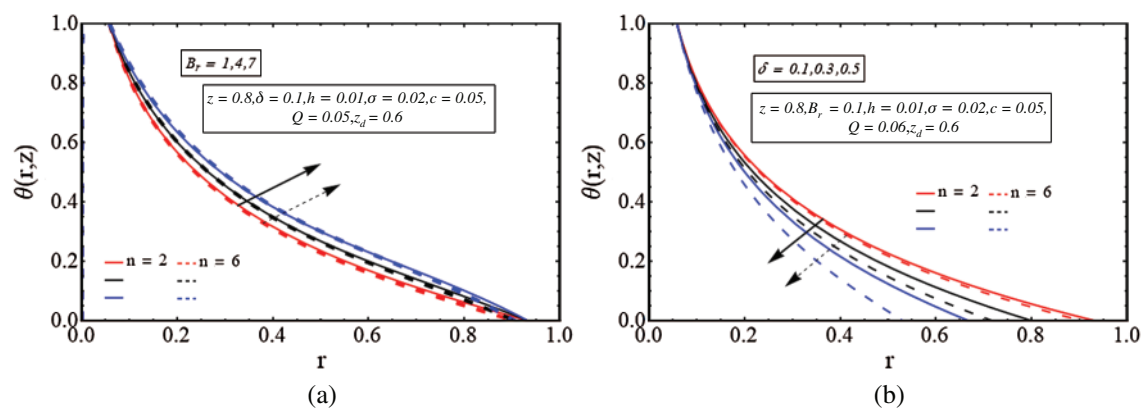


Figure 3: (Continued)

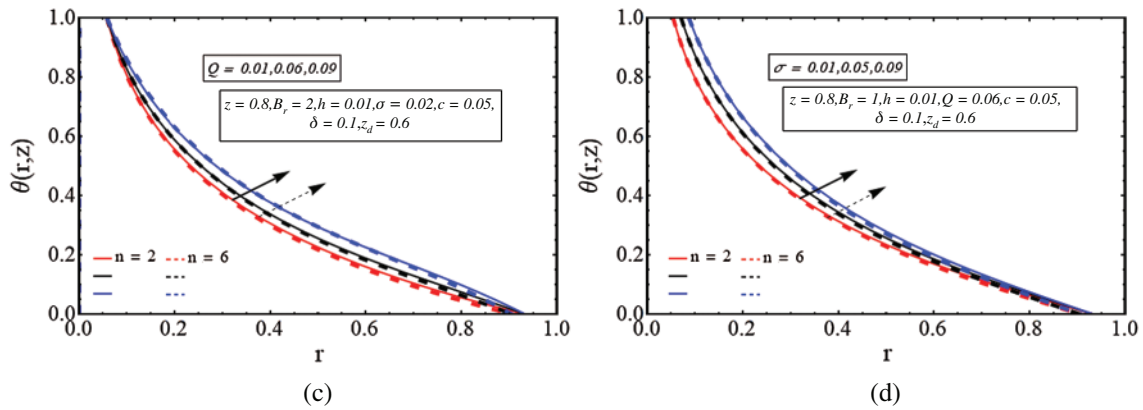


Figure 3: (a) Temperature profile for B_r . (b) Temperature profile for δ . (c) Temperature profile for Q . (d) Temperature profile for σ

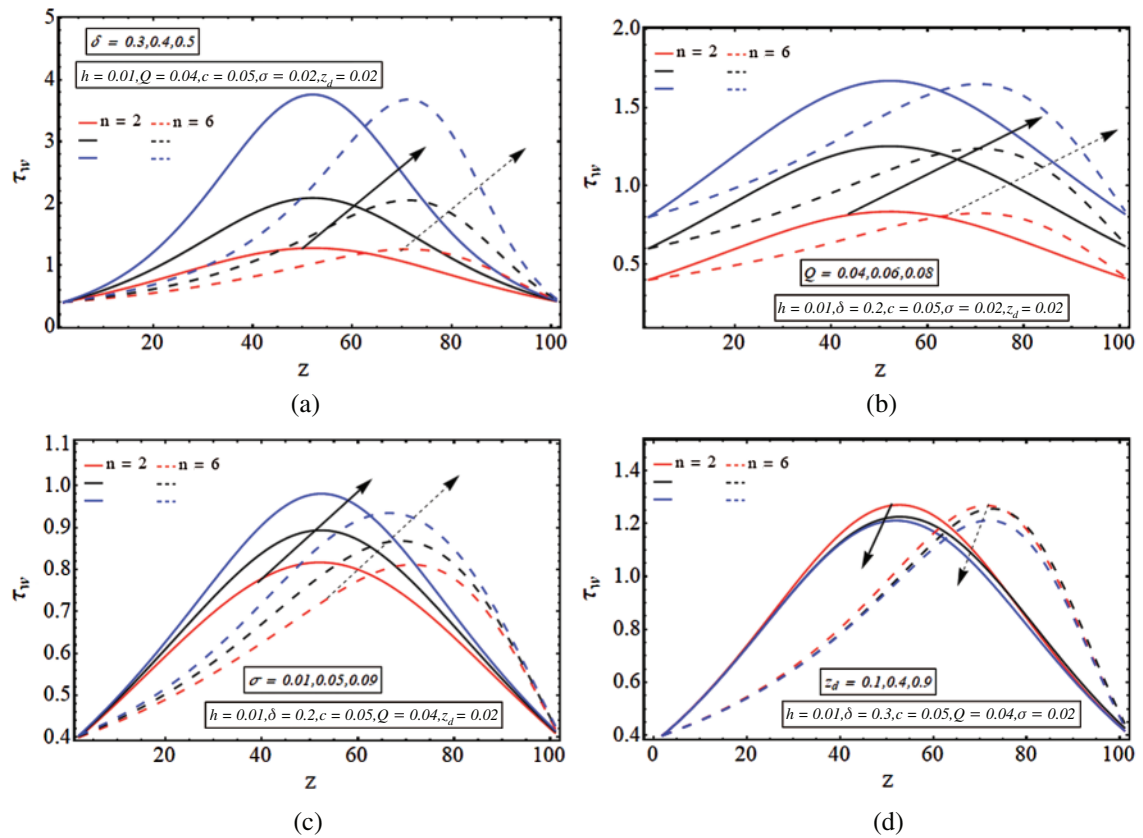


Figure 4: (a) Wall shear stress for δ . (b) Wall shear stress for Q . (c) Wall shear stress for σ . (d) Wall shear stress for z_d

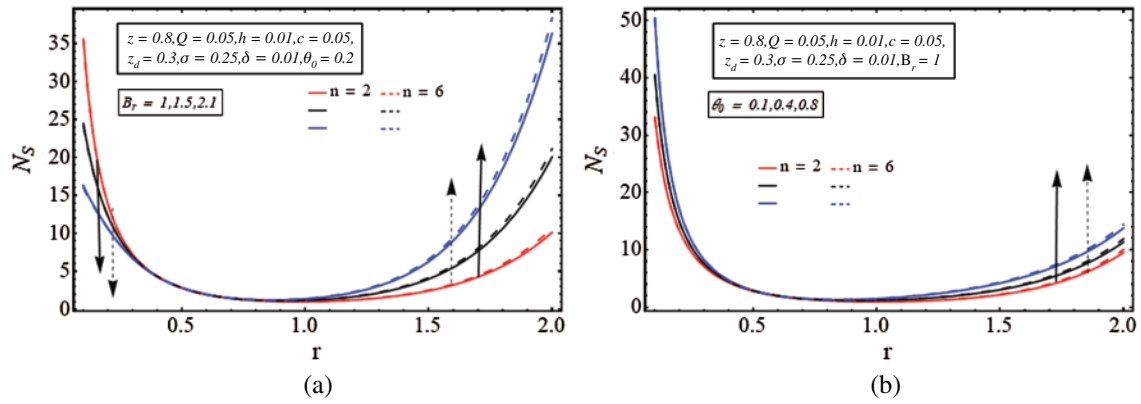


Figure 5: (a) Entropy for B_r . (b) Entropy for θ_0

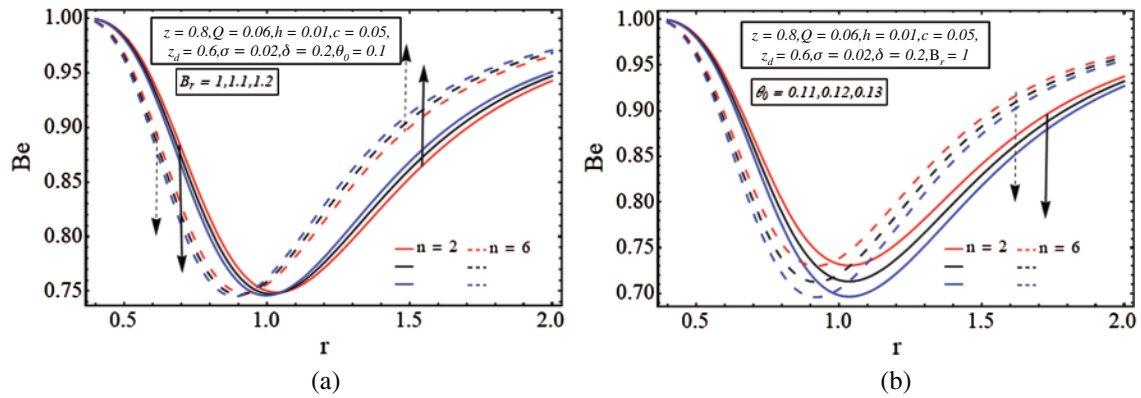


Figure 6: (a) Bejan number for B_r . (b) Bejan number for θ_0

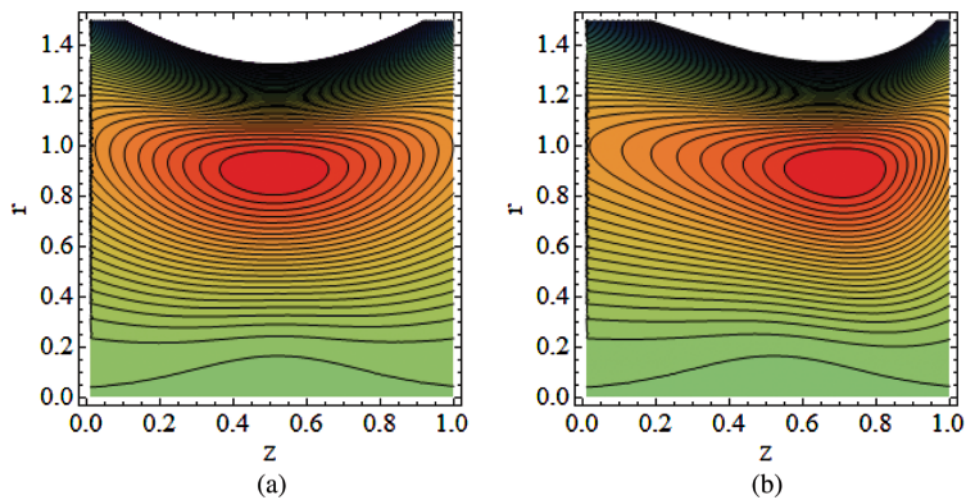


Figure 7: (Continued)

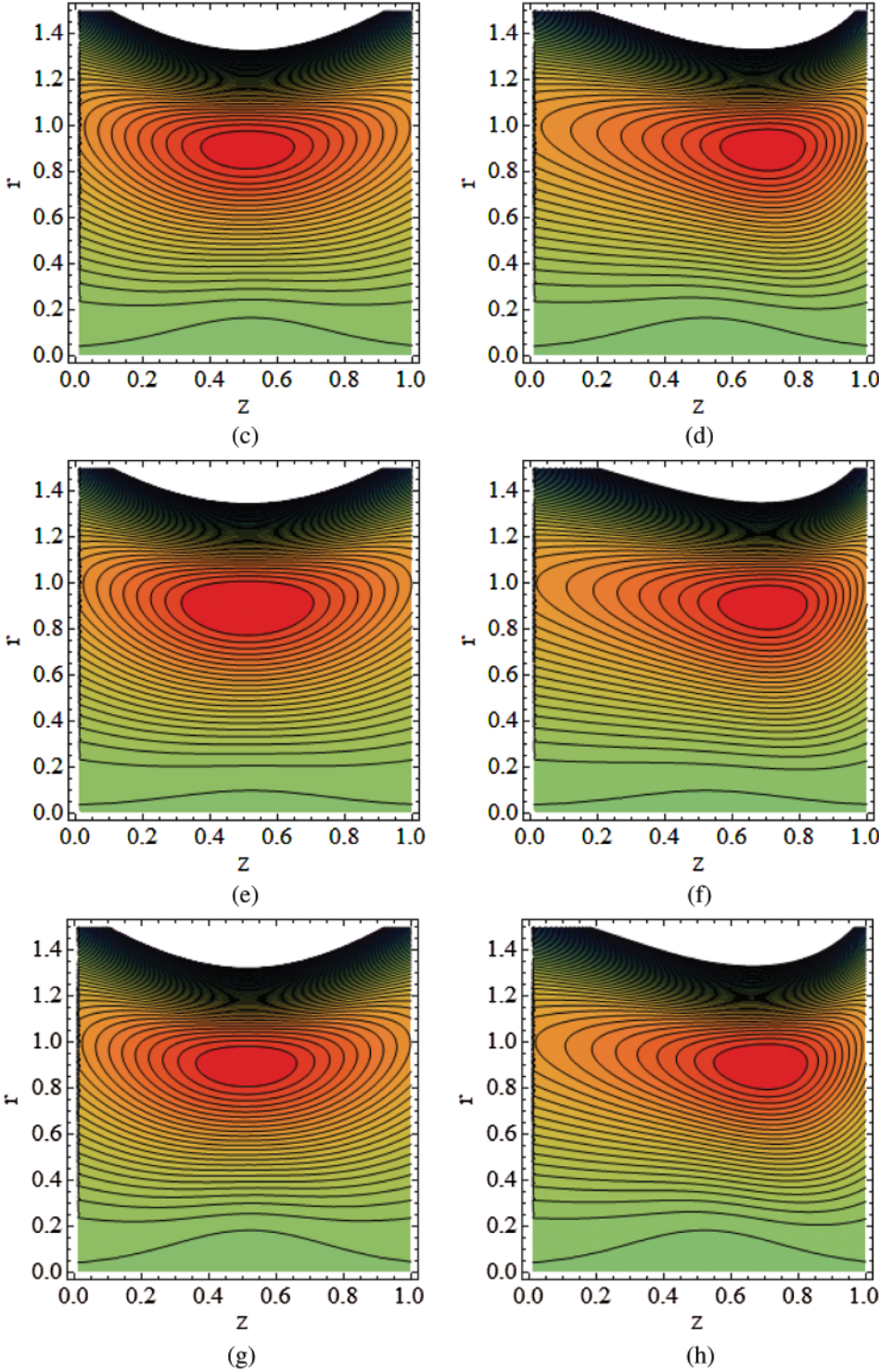


Figure 7: (a) Streamlines for $Q = 1, n = 2$. (b) Streamlines for $Q = 1, n = 6$. (c) Streamlines for $Q = 1.3, n = 2$. (d) Streamlines for $Q = 1.3, n = 6$. (e) Streamlines for $\sigma = 0.04, n = 2$. (f) Streamlines for $\sigma = 0.04, n = 6$. (g) Streamlines for $\sigma = 0.09, n = 2$. (h) Streamlines for $\sigma = 0.09, n = 6$

6 Conclusions

The blood flow through a catheterized artery having a stenosed wall together with a blood clot at the centre of artery is studied. Stenosis can occur in vessels carrying blood to brain (i.e., Carotid arteries), Renal arteries that supply blood to kidneys etc. The flow is refined in such vessels by application of catheter. The major findings are

- When the height of mild stenosis increases, and the channel becomes narrow then the velocity increases in the centre, but it decreases with the stenosed wall.
- When the height of blood clot σ increases then the velocity of blood flow reduces with the wall having clot, but it remains almost same with the stenosed wall.
- The velocity quickly increases for a non-symmetric stenosis as compared to a symmetric stenosis.
- There is more resistance to flow at the wall with stenosis when the height of stenosis increases.
- There is an increase in entropy with enhancing values of B_r for both cases of symmetric and non-symmetric shapes of stenosis.
- The trapping is symmetric for a symmetric stenosis shape, but it changes to non-symmetric trapping when we have a non-symmetric shape of stenosis.

Funding Statement: The author(s) received no specific funding for this study.

Conflicts of Interest: The authors declare that they have no conflicts of interest to report regarding the present study.

References

1. Ponalagusamy, R. (1986). *Blood flow through stenosed tube (Doctoral dissertation, Ph.D. Thesis)*. IIT Bombay, India.
2. Chaturani, P., Ponnalagar Samy, R. (1985). A study of non-Newtonian aspects of blood flow through stenosed arteries and its applications in arterial diseases. *Biorheology*, 22(6), 521–531. DOI 10.3233/BIR-1985-22606.
3. Nadeem, S., Akbar, N. S., Hendi, A. A., Hayat, T. (2011). Power law fluid model for blood flow through a tapered artery with a stenosis. *Applied Mathematics and Computation*, 217(17), 7108–7116. DOI 10.1016/j.amc.2011.01.026.
4. Ellahi, R., Rahman, S. U., Gulzar, M. M., Nadeem, S., Vafai, K. (2014). A mathematical study of non-Newtonian micropolar fluid in arterial blood flow through composite stenosis. *Applied Mathematics & Information Sciences*, 8(4), 1567–1573. DOI 10.12785/amis/080410.
5. Ellahi, R., Ur-Rahman, S., Nadeem, S. (2013). Analytical solutions of unsteady blood flow of Jeffery fluid through stenosed arteries with permeable walls. *Zeitschrift für Naturforschung A*, 68(8–9), 489–498. DOI 10.5560/zna.2013-0032.
6. Doffin, J., Chagneau, F. (1981). Oscillating flow between a clot model and a stenosis. *Journal of Biomechanics*, 14(3), 143–148. DOI 10.1016/0021-9290(81)90020-8.
7. Srivastava, V. P., Rastogi, R. (2010). Blood flow through a stenosed catheterized artery: Effects of hematocrit and stenosis shape. *Computers & Mathematics with Applications*, 59(4), 1377–1385. DOI 10.1016/j.camwa.2009.12.007.
8. Mekheimer, K. S., El Kot, M. A. (2012). Mathematical modeling of axial flow between two eccentric cylinders: Application on the injection of eccentric catheter through stenotic arteries. *International Journal of Non-Linear Mechanics*, 47(8), 927–937. DOI 10.1016/j.ijnonlinmec.2012.03.005.
9. Ramana Reddy, J. V., Srikanth, D., Krishna Murthy, S. V. S. S. N. V. G. (2014). Mathematical modelling of pulsatile flow of blood through catheterized unsymmetric stenosed artery—Effects

- of tapering angle and slip velocity. *European Journal of Mechanics-B/Fluids*, 48, 236–244. DOI 10.1016/j.euromechflu.2014.07.001.
10. Bhatti, M. M., Zeeshan, A., Ellahi, R. (2016). Heat transfer analysis on peristaltically induced motion of particle-fluid suspension with variable viscosity: Clot blood model. *Computer Methods and Programs in Biomedicine*, 137, 115–124. DOI 10.1016/j.cmpb.2016.09.010.
 11. Ahmed, A., Nadeem, S. (2017). Shape effect of Cu-nanoparticles in unsteady flow through curved artery with catheterized stenosis. *Results in Physics*, 7, 677–689. DOI 10.1016/j.rinp.2017.01.015.
 12. Akbar, N. S., Raza, M., Ellahi, R. (2016). Endoscopic effects with entropy generation analysis in peristalsis for the thermal conductivity of 2 HO nanofluid. *Journal of Applied Fluid Mechanics*, 9(4), 1721–1730. DOI 10.18869/acadpub.jafm.68.235.24422.
 13. Akbar, N. S., Butt, A. W. (2017). Entropy generation analysis in convective ferromagnetic nano blood flow through a composite stenosed arteries with permeable wall. *Communications in Theoretical Physics*, 67(5), 554. DOI 10.1088/0253-6102/67/5/554.
 14. Liu, Q., Chen, L. (2020). Time-space fractional model for complex cylindrical ion-acoustic waves in ultrarelativistic plasmas. *Complexity*, 2020, 9075823, 16. DOI 10.1155/2020/9075823.
 15. Jayaraman, G., Sarkar, A. (2005). Nonlinear analysis of arterial blood flow—steady streaming effect. *Nonlinear Analysis: Theory, Methods & Applications*, 63(5–7), 880–890. DOI 10.1016/j.na.2005.01.016.
 16. Bejan, A. (1979). A study of entropy generation in fundamental convective heat transfer. *Journal of Heat Transfer*, 101(4), 718–725.
 17. Akbar, N. (2015). Entropy generation analysis for a CNT suspension nanofluid in plumb ducts with peristalsis. *Entropy*, 17(3), 1411–1424. DOI 10.3390/e17031411.